EXACT CONTINUUM SOLUTION FOR A CHANNEL THAT CAN BE OCCUPIED BY TWO IONS

DAVID G. LEVITT
Department of Physiology, University of Minnesota, Minneapolis, Minnesota 55455

ABSTRACT The classical Nernst–Planck continuum equation is extended to the case where the channel can be occupied simultaneously by two ions. A two-dimensional partial differential equation is derived to describe the steady-state channel. This differential equation is of the form of the generalized Laplace equation, but it has the novel feature that the boundary conditions are periodic. The finite difference solution takes ~8 s on a large computer. The equations are solved for the special case of a cylindrical channel with a fixed charge in the center. It is assumed that the forces on the ions result entirely from the sum of the Born image potential, the fixed charge potential, the interaction potential between the two ions, and the applied voltage. Approximate simple analytical expressions are derived for these potential terms, based on the assumption that the electric field perpendicular to the channel wall is zero. The potentials include the contribution from a diffuse charge (Debye–Huckel) reaction field in the bulk solution. The solution for the monovalent cation flux was obtained for channels with a radius of 4 Å and lengths of 16 and 32 Å and a fixed charge valence of -1 and -1.5. For these channels, a significant fraction (up to 90%) of the total resistance is contributed by the bulk solution and results were obtained for the case where the "channel" included 8 Å of bulk solution at each channel end. These results for the two-ion channel were compared with the analytical solution for a one-ion channel. The one-ion channel is a fair approximation to the two-ion channel for a fixed charge of -1, underestimating the flux at high concentrations by ~ 30%. However, for a fixed charge of -1.5, the one-ion model is a poor approximation, with the two-ion flux about seven times that of the one-ion model at high concentrations. The absolute conductance and concentration dependence of these channels (with a fixed charge of -1) mimic the behavior of the large conductance K^+ channel and the acetylcholine receptor channel.

INTRODUCTION

The Nernst–Planck continuum model provides a simple and elegant description of the flux of ions through cell membrane channels in terms of three parameters: the diffusion coefficient, the cross-sectional area, and the energy profile of the ion in the channel (Levitt, 1986). Its main limitation (and the reason it is rarely used to model biological channels) is that it is only applicable to situations in which there is a high probability that the channel is empty. If another ion was already in the channel, it would alter the energy profile which would now become a complicated function of the position of the two ions. Although a number of approximate solutions for the multi-ion case have been developed (Levitt, 1986), there has not, as yet, been a complete solution for the case in which there is more than one ion in the channel. The purpose of this paper is to present a general solution for the case of a channel that can be occupied by at most two ions.

The most important application of this two-ion continuum solution is for situations in which the forces are dominated by long range electrostatic effects and it should be particularly useful for modeling the transport up to the channel mouth in the bulk solution. The use of this solution will be illustrated by applying it to a uniform cylindrical channel that contains a fixed charge in its center. It will be assumed that the energy profile arises entirely from the sum of the potential from the fixed charge, the Born image potential, and the interaction between the two ions. Simple analytical expressions for these potentials are derived using the assumption that the electric field perpendicular to the channel wall is zero (Levitt, 1985). This potential includes the contribution from a diffuse charge (Debye–Huckel) reaction field in the bulk solution. The inclusion of this reaction field means that the model is slightly more general than a "two-ion" channel since it does allow in an approximate way for the presence of additional ions in the bulk solution. The "channel" includes the bulk solution regions that contribute to the overall channel resistance. The first section describes the derivation of the general partial differential equation (and boundary conditions) for the two-ion channel; the second section describes the derivation of the analytical expressions for the electrostatic potentials and the restricted cross-sectional area; and the last section describes the application of the theory to the cylindrical channel.

Address correspondence to David G. Levitt, Department of Physiology, 6-255 Millard Hall, 435 Delaware Street SE, University of Minnesota, Minneapolis, MN 55455.

GLOSSARY

a	radius of channel
B	radius of ion
X	position along channel axis
M, L	half length of channel and of channel plus bulk solution
$S(X)$	electrostatic cross-sectional area
$S_e(X)$	restricted cross-sectional area available to the ion
$C(X), C_0$	concentration (number/cm^3) at X and in bulk solution
ϵ_w	dielectric constant of water
e	electron charge
E	electron field
Φ	electric potential
Ψ_1	applied voltage
U_B, U_F, U_I, U_T	potential energy from Born image, fixed charge, ion interaction, and total energy

Dimensionless Variables

$x = X/a$; $b = B/a$; $m = M/a$; $s = S/a^2$; $c = a^3C$; $\gamma = e^2/(\epsilon_w kTa) = 6.96/a(\text{Å})$; $z = q/e$; $\lambda = (8\pi\gamma c_o)^{1/2}$; $\psi = ze\Psi/kT$; $\phi = \Phi/(e/\epsilon_w a)$; $\zeta = E/(e/\epsilon a^2)$; $u = U/(e^2/\epsilon_w a)$; $w = U/kT = \gamma u$

GENERAL SOLUTION FOR THE ION FLUX THROUGH A TWO-ION CHANNEL

The derivation consists of five parts: (*a*) The derivation of the partial differential equation for $P(X, Y)$, the probability density function for the case that one ion is at X while the other ion is at Y. (*b*) Derivation of the boundary condition for the differential equation. (*c*) Since the solution is first obtained for $P(X, Y)$ normalized by P_0 (the probability the channel is empty), it is necessary to derive an expression for P_0 to obtain the (unnormalized) $P(X, Y)$. (*d*) Derivation of the flux equation in terms of $P(X, Y)$. (*e*) Numerical solution.

Differential Equation for $P(X, Y)$

The fundamental function is $P(X, Y)$, the probability density function for one ion at X and the other at Y. The dimension of P is (length)$^{-2}$. It will be assumed that the two ions are identical (i.e, only one type of permeable ion is present) so that the constraint $X \le Y$ can be imposed. A steady state will be assumed:

$$\frac{\partial P}{\partial t} = 0 = -\frac{\partial}{\partial X}(V_X P) - \frac{\partial}{\partial Y}(V_Y P). \tag{1}$$

This is just the continuity equation in the two-dimensional (X, Y) space where V_X and V_Y are the phase space velocities in the X and Y directions. Expressions for these velocities can be obtained from the following argument. Define $J(X; Y)$ and $C(X; Y)$ as the number flux and concentration (No. of ions per unit vol) at X if an ion is at Y.

$$\begin{aligned} J(X; Y) &= C(X; Y)S_e(X)V_X \\ &= -D(X)S_e(X)\left[\frac{\partial C(X; Y)}{\partial X} + C(X; Y)\frac{\partial w(X, Y)}{\partial X}\right], \end{aligned} \tag{2}$$

where $S_e(X)$ is the cross-sectional area available to the ion, D is diffusion coefficient, and $w(X, Y)$ is the total dimensionless energy of the two-ion channel system (normalized by kT; $U = kTw$). The first equality is simply the definition of V_X, whereas the second equality is the classical Nernst–Planck equation (Levitt, 1986) with the second ion fixed at Y. Defining $P(X; Y)$ (of dimension 1/length) as the probability density of finding an ion at X if an ion is at Y:

$$C(X; Y)S_e(X) = P(X; Y) = P(X, Y)/P_1(Y). \tag{3}$$

Eqs. 2 and 3 can then be used to solve for $V_X P$ (and a similar expression for $V_Y P$):

$$V_X P(X, Y) = -D(X)\left[S_e(X)\frac{\partial}{\partial X}(P/S_e) + \frac{P\partial w}{\partial X}\right]. \tag{4}$$

Analogous to the procedure used to solve the Nernst–Planck equation, an alternative set of derived functions will be defined:

$$\begin{aligned} p(X, Y) &= P(X, Y)/S_e(X)\,S_e(Y) \\ H(X, Y) &= S_e(X)\,S_e(Y)e^{-w} \\ F(X, Y) &= e^{w}p(X, Y). \end{aligned} \tag{5}$$

Substituting Eq. 4 (in terms of these derived functions) into Eq. 1, one obtains the final form of the fundamental differential equation describing the two-ion channel:

$$\frac{\partial}{\partial X}\left[D(X)H(X, Y)\frac{\partial F}{\partial X}\right] + \frac{\partial}{\partial Y}\left[D(Y)H(X, Y)\frac{\partial F}{\partial Y}\right] = 0. \tag{6}$$

Boundary Conditions

The boundary conditions for this equation present an interesting problem. The length of the "channel" (including the bulk solution) will be defined as $2L$ with the channel ends at $X = -L$ and $X = L$. (The length of the physical channel is $2M$, with $M \le L$.) Eq. 6 is of the form of the generalized Laplace equation and usually requires either that F or its derivative (or a combination of the two) be prescribed on the boundary (X, L) and $(-L, Y)$, corresponding to knowing the probability of finding one ion, e.g., at $X = -L$ (the channel end) when the other ion is at Y (an arbitrary channel position). However, all that is actually known is the concentration in the bulk solution, which corresponds to the value of P (or F) at only one point. The solution to this problem results from the observation that

one can derive the following set of periodic boundary conditions that lead to a unique solution.

The fundamental assumption leading to the derivation of the boundary condition (and the crucial assumption for the model) is that the ions at the "channel" ends are in equilibrium with the bulk solution. The "channel" includes the bulk solution regions that limit the flux. This assumption requires that the "channel" be extended far enough into the bulk solution that the rate that ions exchange between the "channel" end and the bulk solution is fast compared with the rate of transport through the channel. This is equivalent to the requirement that the "channel" includes all of the bulk solution that limits the rate of transport. This assumption is the major limitation of the model. Clearly, this assumption will be satisfied if one extends the channel region far enough into the bulk solution. However, if too much bulk solution is included, the condition that the channel contains at most two ions will be violated. The actual channel length that is used must be a compromise between these two competing requirements.

The first boundary condition arises from the condition that there is equilibrium binding of the second ion at the channel end. The binding reaction at the left end can be written as

$$C_1 + p_1(X) \leftrightarrow p(-L, X), \tag{7}$$

where C_1 is the concentration in the bulk solution on the left side and $p_1(X)S_e(X)$ is the probability of finding only one ion in the channel (at X) and p_1 is equivalent to the concentration at X. Since this reaction is assumed to be at equilibrium, the equilibrium constant can be written in terms of the free energy difference:

$$p(-L, X) = C_1 p_1(X) e^{-[w(-L,X)-w(X)-\psi_1]}, \tag{8}$$

where $w(X)$ and $w(-L, X)$ are the energy of the one- and two-ion channel, respectively, and $ze\Psi_1$ is the energy of the ion (valence z) in the left bulk solution which has a dimensionless voltage $\psi_1 = ze\Psi_1/kT$. One can derive a similar relation for the right end:

$$P(X, L) = C_2 p_1(X)\, e^{-[w(X,L)-w(X)]}. \tag{9}$$

(The voltage has been defined to be equal to zero for the bulk solution on the right side.) Taking the ratio of Eqs. 8 and 9 and using the definition of F (Eq. 5) leads to one periodic boundary condition:

$$F(X, L) = (C_2/C_1)\, e^{-\psi_1} F(-L, X). \tag{10}$$

Binding of the first ion to the right channel end can be described by

$$C_2 + P_0 \leftrightarrow p_1(L), \tag{11}$$

where P_0 is the probability that the channel is empty. From the assumption of equilibrium at the channel end:

$$p_1(L) = C_2 P_0\, e^{-w(L)}. \tag{12}$$

Combining Eqs. 8 and 12,

$$F(-L, L) = C_1 C_2 e^{\psi_1} P_0 \tag{13a}$$

Also, using Eq. 10,

$$F(L, L) = C_2^2 P_0; \quad F(-L, -L) = C_1^2 e^{2\psi_1} P_0. \tag{13b,c}$$

Eqs. 13 represent the only points at which $F(X, Y)$ has a definite prescribed value; the rest of the boundary conditions are periodic.

A second periodic boundary condition arises from the steady-state condition for the one-ion channel, which can be written in the form

$$\frac{\partial P_1(X)}{\partial t} = 0$$

$$= -\frac{d}{dX}[V_1 P_1(X)] - V_{-L} P(-L, X) + V_L P(X, L). \tag{14}$$

The first term on the right represents the flux at X in a channel that contains one ion, whereas the last two terms represent the rate at which the one-ion channel is converted into a two-ion channel by ions entering or leaving the channel ends. These three terms can be written as

$$J_1 = V_1 P_1(X) = -D(X) H_1(X) \frac{d}{dX}(p_1 e^{w_1})$$

$$= -D(X) H_1(X) C_1^{-1} e^{-\psi_1} \frac{d}{dX} F(-L, X)$$

$$V_{-L} P(-L, a) = -D(-L) H(-L, X) \frac{\partial}{\partial(-L)} F(-L, X)$$

$$V_L P(X, L) = -D(L) H(X, L) \frac{\partial}{\partial L} F(X, L). \tag{15}$$

Substituting these expressions into Eq. 14, one obtains another set of periodic boundary conditions:

$$(e^{-\psi_1}/C_1) \frac{d}{dX}\left[D(X) H_1(X) \frac{d}{dX} F(-L, X)\right]$$

$$= D(L) H(X, L) \frac{\partial}{\partial L} F(X, L) - D(-L) H(-L, X)$$

$$\frac{\partial}{\partial(-L)} F(-L, X). \tag{16}$$

The final boundary condition that needs to be prescribed is along the line $X = Y$. It will be assumed that the two ions cannot pass each other in the channel and therefore, the potential energy of interaction (U_I) must go to infinity when $X = Y$. However, such a steep potential at $X = Y$ would complicate the numerical solution and, instead, the

"no pass" condition is imposed as a boundary condition at $X = Y$:

$$\frac{\partial}{\partial X} F(X, Y) = 0 \text{ at } X = Y. \tag{17}$$

The two-ion channel is now uniquely described by the partial differential Eq. 6 along with the boundary conditions of Eqs. 10, 13, 16, and 17.

The equations are simplified if they are rewritten in terms of a set of dimensionless functions normalized by a (the channel radius) and D_0 (the bulk diffusion coefficient). These functions and a complete set of equations describing the two-ion channel are summarized below:

$$x = X/a, \ell = L/a, s_c = S_c/a^2,$$

$$c = a^3C, \Delta = D/D_0, h = H/a^4, h_1 = H_1/a^2,$$

$$f = F/(P_0C_1C_2e^{\psi_1}), \beta = (c_2/c_1)e^{-\psi_1}$$

$$\frac{\partial}{\partial x}\left[\Delta(x)h(x,y)\frac{\partial f}{\partial x}\right] + \frac{\partial}{\partial y}\left[\Delta(y)h(x,y)\frac{\partial f}{\partial y}\right] = 0 \tag{18a}$$

$$f(x, \ell) = \beta f(-\ell, x) \tag{18b}$$

$$(e^{-\psi_1}/c_1)\frac{\mathrm{d}}{\mathrm{d}x}\left[\Delta(x)h_1(x)\frac{\mathrm{d}}{\mathrm{d}x}f(-\ell, x)\right] = \Delta(\ell)h(x, \ell) \cdot \frac{\partial}{\partial \ell}f(x, \ell) - \Delta(-\ell)h(-\ell, x)\frac{\partial}{\partial(-\ell)}f(-\ell, x) \tag{18c}$$

$$\frac{\partial}{\partial x}f(x\,y) = 0 \text{ at } x = y \tag{18d}$$

$$f(-\ell, \ell) = 1; f(-\ell, -\ell) = 1/\beta; f(\ell, \ell) = \beta. \tag{18e}$$

Expression for P_0

In Eq. 18, F has been normalized by P_0 (the probability the channel is empty) so that P_0 has dropped out of the boundary condition (see Eq. 13). The solution will first be obtained for f, from which P_0 (and then F) will be determined. The value of P_0 is determined from the condition that the channel can hold a maximum of two ions:

$$1 = P_0 + P_1 + P_2 = P_0(1 + M_1 + M_2), \tag{19}$$

where P_0, P_1, and P_2 are the probability that the channel contains zero, one, or two ions. The expressions for M_1 and M_2 can be obtained by integrating over $f(x, y)$ (see Eq. 8 for definition of P_1).

$$P(x, y) = a^{-2}h(x, y)P_0c_1c_2e^{\psi_1}f(x, y)$$

$$P_1(x) = a^{-1}c_2h_1(x)P_0f(-\ell, x)$$

$$M_1 = \int_{-L}^{L} P_0^{-1}P_1(X)\mathrm{d}X = c_2\int_{-\ell}^{\ell} h_1(x)f(-\ell, x)\,\mathrm{d}x$$

$$M_2 = c_1c_2e^{\psi_1}\int_{-\ell}^{\ell}\mathrm{d}y\int_{-\ell}^{y} h(x, y)f(x, y)\,\mathrm{d}x. \tag{20}$$

Flux Equation

The only theoretical value that can be measured experimentally is the channel flux. The flux at position X [$J(X)$] in the channel is the sum of two terms:

$$J(X) = J_1(X) + J_2(X),$$

where J_1 and J_2 are the flux in a channel that contains one or two ions. J_1 is described by Eq. 15 and the expression for J_2 is obtained by integrating over all possible positions of the second ion:

$$J_2(X) = \int_{-L}^{X} P(\alpha, X)V_X\mathrm{d}\alpha + \int_{X}^{L} P(X, \alpha)\,V_X\mathrm{d}\alpha$$

$$= -\int_{-L}^{X} D(X)H(\alpha, X)\frac{\mathrm{d}}{\mathrm{d}X}F(\alpha, X)\,\mathrm{d}\alpha - \int_{X}^{L} D(X)H(X, \alpha)\frac{\mathrm{d}}{\mathrm{d}X}F(X, \alpha)\mathrm{d}\alpha.$$

Although these expressions could be used to determine the theoretical flux, they have two disadvantages. First, they require an accurate numerical derivative of the numerical solution $F(x, y)$, a procedure that is inherently inaccurate. Second, it only uses the value of $F(x, y)$ at a single point or set of points, throwing away much of the information obtained in the solution.

A better approach makes use of the fact that in the steady state, the flux must be independent of position. That the above solution does satisfy this condition can be shown as follows: The derivative of the total flux at X is described by

$$\frac{\mathrm{d}J(X)}{\mathrm{d}X} = \frac{\mathrm{d}}{\mathrm{d}X}[V_1P_1(X)] + \frac{\mathrm{d}}{\mathrm{d}X} \cdot \int_{-L}^{X} \mathrm{P}(\alpha, X)V_X\mathrm{d}\alpha + \frac{\mathrm{d}}{\mathrm{d}X}\int_{X}^{L} P(X, \alpha)V_X\mathrm{d}\alpha. \tag{21}$$

The second term can be expanded as

$$P(X, X)V_X + \int_{-L}^{X}\frac{\mathrm{d}}{\mathrm{d}X}[P(\alpha, X)V_X]\mathrm{d}\alpha. \tag{22}$$

Integrating Eq. 1 from $\alpha = -L$ to $\alpha = X$,

$$V_{-L}P(-L, X) - V_XP(X, X) = \int_{-L}^{X}\frac{\partial}{\partial X}[V_XP(\alpha, X)]\mathrm{d}\alpha. \tag{23}$$

Substituting Eq. 23 and Eq. 22 for the second term in Eq. 21 (and similar expressions for the third term) and using the boundary condition Eq. 14 yields the result that the derivative of the flux (Eq. 21) is zero, i.e., the flux is independent of position.

Since the flux does not depend on x, it is equal to the flux averaged over the length of the channel, now written in dimensionless form $j = a^2J/(P_0D_0c_2)$:

$$j = (2\ell)^{-1}\int_{-\ell}^{\ell}[j_1(x) + j_2(x)]\mathrm{d}x. \tag{24}$$

The two terms in Eq. 24 can be obtained by integrating the expressions for J_1 and J_2 by parts:

$$2\ell j = \int_{-\ell}^{\ell} f(-\ell, x) \frac{d}{dx} [h_1(x)\Delta(x)]dx + \Delta(-\ell)h_1(-\ell) f(-\ell, -\ell) - \Delta(\ell)h_1(\ell) f(-\ell, \ell) + c_1 e^{-\psi} \left\{ \int_{-\ell}^{\ell} \left[\int_{-\ell}^{x} f(\alpha, x) \frac{\partial}{\partial x} [\Delta(x)h(\alpha, x)] \, d\alpha + \int_{x}^{\ell} f(x, \alpha) \frac{\partial}{\partial x} [\Delta(x)h(x, \alpha)]d\alpha - h(x, \ell)\Delta(\ell) f(x, \ell) + h(-\ell, x) \cdot \Delta(-\ell) f(-\ell, x) \right] dx \right\}. \quad (25)$$

This expression for the flux is now in terms of an integral over the numerical solution $f(x, y)$. It is a function of the partial derivative of the potential energy function $h(x, y)$ $(= s_e(x)s_e(y)e^{-w})$. In the specific example discussed below, analytical expressions are obtained for s_e and w so that the derivative is known exactly.

This completes the derivation of the general theory. The differential equation and boundary conditions for the normalized function $f(x, y)$ is described by Eq. 18. Knowing $f(x, y)$, the value of P_0 can then be determined from Eqs. 19 and 20. The absolute probability density function $P(X, Y)$ can then be determined using the definitions of f (Eq. 18) and F (Eq. 5). The normalized flux (j) is determined from Eq. 25 using $f(x, y)$ and the absolute flux can then be determined from the definition of j (see Eq. 24) and knowledge of P_0.

Numerical Solution

The partial differential equation (Eq. 18) is solved by a finite difference method which leads to an unsymmetric large sparse matrix that must be inverted (see Appendix). This matrix can become quite large. For example, if the channel is divided into 48 intervals, then the function $f(x, y)$ must be determined at $48^2/2$ or 1,152 different positions (the division by two results from the condition that $x \le y$). That is, one must invert an 1,152 by 1,152 matrix. There are two fundamentally different approaches to solving large sparse matrices, iterative and exact. The iterative approach has the advantage of small memory requirements, simplicity, and (when it converges rapidly) speed. A number of iterative techniques (Hageman and Young, 1981) were tried, including line successive overrelaxation (LSOR), alternating direction method and two modified conjugate gradient methods (Young and Jea, 1980; Saad, 1982). Although the LSOR was the best of those tried, its rate of convergence became hopelessly slow for some values of the potential function, seriously limiting its general usefulness. Thus, I have chosen to use an exact sparse matrix procedure (the Yale Sparse Matrix Program [YSMP] which is implemented on most large computers). The computer time is not long (about the same as for the interative approach when it converges slowly) but it is quite demanding of memory. For the 48-interval example, the YSMP solution takes ~8 s on the Cyber 845 and requires a one-dimensional working array of dimension 72,000.

POTENTIAL ENERGY AND RESTRICTED AREA FUNCTIONS

This general solution is in terms of the function of $w(x, y)$, which is the total energy of the two ion system. This function contains all the information and physics that uniquely characterizes the channel. One of the advantages of the Nernst–Planck approach is that it allows a general solution of this form to be obtained. However, to apply the solution to a specific channel, the function $w(x, y)$ must be specified. In this section, it will be assumed that $w(x, y)$ is due entirely to long range electrostatic effects and an approximate analytical expression will be obtained. In the next section, this expression will be used to illustrate a specific solution to the general equations. In addition to providing this illustrative example, it is hoped that this analytical expression summarizes the most important contributions to $w(x, y)$ and will be useful in other problems.

An exact solution for the electrostatic potential energy function $[U(X\,Y) = kTw(x, y)]$ requires an involved numerical solution to obtain the potential at a single point (Levitt, 1978). To obtain an accurate value for the derivative of the energy (as is required in the flux Eq. 25), it would be necessary to makes these calculations at thousands of points. The purpose of this section is to derive an analytical approximation for this exact numerical result.

The fundamental assumption (see Levitt [1985] for details) that allows one to derive simple analytical expressions is the condition that the electric field perpendicular to the channel wall is zero. This condition results from the fact that the dielectric constant of water (78) is much greater than that of the channel wall ($\approx$2). This assumption means that the field lines from the ion at X_1 have the appearance shown in Fig. 1. At each X, the field lines are assumed to be perpendicular to the surface $S(X)$ whose area is equal to

$$S(X) = \begin{cases} \pi a^2 & 0 \le |X| \le M \\ \pi[a^2 + (X - M)^2] & M \le |X| \le M + a \\ 2\pi(X - M)^2 & M + a \le |X|, \end{cases} \quad (26)$$

where a is the radius and M is the half length of the channel. S is the electrostatic surface area and may be larger than the physical area if, for example, the channel is lined by polar (high dielectric) groups. Although the physical length of the channel is $2M$, the actual "channel" region that limits the flux extends out into the bulk solution and is of length $2L$. The channel has axial symmetry and the potential is characterized by the single variable X,

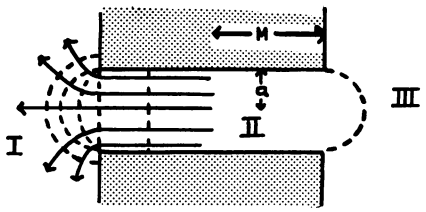

FIGURE 1 Schematic diagram showing the assumed form of the field lines in a channel of half length M and radius a. The dotted lines show the surface areas described by Eq. 26.

which is the axial position within the channel and the radial distance from mouth of chennel in the bulk solution.

The channel is divided into three regions (Fig. 1). In region II ($-a-\mathrm{M} \le X \le a + M$) only the discrete ions are present, whereas in region I ($X \le -a-M$) and III ($a + M \le X$) a diffuse charge (Debye–Huckel) reaction field is included. The potential energy is the sum of four terms: (*a*) the potential from the fixed charge of valence z_f [$U_F(X)$], which is assumed to be in the center of the channel; (*b*) the Born image potential [$U_B(X)$]; (*c*) the potential of interaction between the two ions [$U_I(X, Y)$]; and (*d*) the potential from the externally applied voltage, expressed as the ratio of the voltage at X relative to the applied voltage Ψ_1 (the voltage in the bulk solution on the left side [Ψ_2] is defined to be zero). The details of the derivation of these terms are described in the Appendix and the final results, expressed in dimensionless variables ($x = X/a$; $m = M/a$, $u = U/[e^2/\epsilon_w a]$; $z = ze\Psi/kT$; λ = Debye length; z_f, z_1, z_2 = valence of fixed charge and of ion one and two) for the condition $X \le Y$ are

$$u_F(x) = 2z_f z_1 I(|x|) \tag{27a}$$

$$u_B(x) = z_1^2\{[1 + \alpha(|x|)]I(|x|) - K(|x|)\} \tag{27b}$$

$$u_I(x, y) = 2z_1 z_2[1 \pm \alpha(|x|)]H(y) \tag{27c}$$

$$\psi(x)/\psi_1 = \begin{cases} 0.5\, I(x)/I(0) & x \ge 0 \\ 1 - 0.5I(-x)/I(0) & x \le 0 \end{cases} \tag{27d}$$

$$\alpha(x) = 1 - I(x)/I(0)$$

$$I(x) = \begin{cases} \dfrac{1}{2(1+\lambda)} + \dfrac{\pi}{4} + m - x & 0 \le x \le m \\ \dfrac{1}{2(1+\lambda)} + \dfrac{\pi}{4} + \tan^{-1}(x - m) & m \le x \le m + 1 \\ \dfrac{e^{-\lambda}(x - 1 - m)}{2(1+\lambda)(x - m)} & m - 1 \le x \end{cases}$$

$$H(x) = \begin{cases} I(x) & x \ge 0 \\ 2I(0) - I(-x) & x \le 0 \end{cases}$$

$$K(x) = \begin{cases} 1 & 0 \le x \le m \\ (1 + x - m)^{-1} & m \le x. \end{cases}$$

The expression for u_B (Eq. 27b) differs slightly from that derived previously (Levitt, 1985). The + and − in Eq. 27c are for the case where x is greater or less than zero, respectively. These equations take a simple form for the case there both ions are within the physical channel ($-m \le x, y \le m$):

$$u_F(x)/2z_f z_1 = I(0) - |x| \tag{28a}$$

$$u_B(x)/z_1^2 = I(0) - x^2/I(0) - 1 \tag{28b}$$

$$u_I(x, y)/2z_1 z_2 = I(0) + x - y - xy/I(0) \tag{28c}$$

$$\psi(x)/\psi_1 = 0.5(1 \pm x/I(0)) \tag{28d}$$

$$I(0) = m + \pi/4 + 0.5/(1+\gamma).$$

The approximation for the fixed charge energy (U_F) assumes that the fixed charge is spread uniformly on a disk in the center of the channel. This should be a good approximation to the more physical situation of ring of charge in the center of the channel. For a discrete fixed charge, the radius of the fixed charge and the distance of closest approach of the ion must be specified. This is not necessary for the diffuse charge approximation used here.

The assumption that the electric field perpendicular to the wall is zero leads to an overestimate of the potential because it constrains the field lines to too small an area. The equations have been empirically adjusted by comparing them with the exact numerical results. The best argument is found if all the potential functions (Eqs. 28a–28c) are divided by 1.5. Using this correction, the expression for the image potential [$U_B(x)$] is within 10% of the exact result (Jordan, 1982) for m varying from 1.5 to 5. Fig. 2 shows a comparison of the exact (Levitt, 1978) and approximate (Eq. 28 using the 1.5 correction factor) energy profile for a one- and two-ion channel of radius 3 Å and half length 12.5 Å ($m = 4.17$). Since this channel does not have any fixed charges, the one-ion potential is equal to the image potential. The two-ion potential is the sum of the image potential of each ion plus the interaction potential. It can be seen that the agreement between the modified

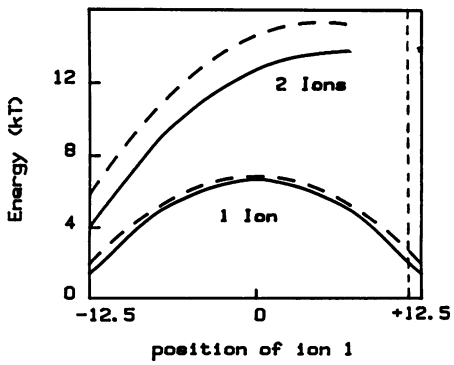

FIGURE 2 Comparison of exact numerical (——) (Levitt, 1978) and approximate analytical (---) (Eq. 27 divided by 1.5) potential energy in a channel with dimensions similar to that of gramicidin (length, 25 Å; radius, 3 Å). The total energy is shown for the case in which there is one or two ions in the channel. For the two-ion case, ion two is at 11.5 Å (---) and ion one is at a variable position.

theory and the exact solution is quite good, especially when compared with the other uncertainties in the problem (e.g., the value of the dielectric constant for the water in the channel and the "effective" dielectric radius of the channel). This approximation should be better for the channels used in this paper which are wider and shorter than the channel used for the comparison in Fig. 2. This modification of Eq. 27 (division of the potentials by 1.5) will be used in the rest of this paper. (In this comparison, the diffuse charge was neglected [$\lambda = 0$] since that is the assumption used for the exact calculations).

The area (S_e) term that enters the fundamental flux equation (Eq. 2) is the cross-sectional area of the "channel" region that is available to the ion. This is less than the physical area because of the finite size of the ion. This was determined by finding the area available to the center of the ion, both within the physical channel and in the bulk solution at the channel mouth. The final result in dimensionless terms ($s_e = S_e/a^2$) is (see Appendix, Eqs. 13A, 16A, and 17A):

$$s_e = \begin{cases} \pi(1-b)^2 & 0 \le |x| \le m \\ \pi[(1-b)^2 + (x-m)^2(1-b^2)] & m \le |x| \le m+1 \\ 2\pi(x-m)(x-m-b) & m+1 \le |x| \end{cases} \quad (29)$$

$$b = (B + a - a_p)/a,$$

where B is the ion radius and a_p is the physical pore radius.

Because of the finite size of the ion, the diffusion coefficient (D) should also vary with position in the channel. Although continuum expressions have been derived for this reduction in D for infinitely long cylindrical channels (Levitt, 1985), these are not applicable to the short channels considered here (length/radius ratio of 2 to 4). Because of the lack of an exact analytical result and to simplify the calculations, it will be assumed here that D is equal to the bulk solution value everywhere in the channel. Since D enters the equations everywhere as the product DS_e, this assumption is equivalent to placing all the reduction in this product in the term S_e, characterized by the parameter b.

APPLICATION TO CYLINDRICAL CHANNEL

To illustrate this approach, the equations will be solved for a uniform cylindrical channel with a fixed charge (valence z_f) in its center. Three different channels will be considered. For all the channels it will be assumed that the electrostatic radius (a) is 4 Å. If the channel were lined by high dielectric polar groups, this would correspond to a physical pore radius of ~3 Å (Jordan, 1984). Only monovalent cations will be considered and it will be assumed that their diffusion coefficient is 1×10^{-5} cm^2/s and b is 0.5, corresponding to an ion radius (B) of ~1 Å (Eq. 29). Two of the channels have a length of 16 Å (half length = M = 8 Å; $m = M/a = 2$), one with $z_f = -1$ and the other with $z_f = -1.5$. The third channel has a length of 32 Å ($m = 4$) and fixed charge of -1. All the solutions presented here were for the case when the channel was divided into 48 equidistant points in the difference method solution (see Appendix). The results were checked by comparing them with the analytical solutions for both the one-ion channel in the law concentration limit and the no interaction solution for the case when $U_I = 0$ (see Appendix). In both cases, the numerical and analytical solutions agreed to better than 1%.

The first question that must be decided is how much bulk solution should be included as part of the "channel." As discussed above, this decision represents a compromise between including all the bulk solution that might limit the conductance, while not making the "channel" so large that the assumption that it contains a maximum of two ions becomes seriously violated. The contribution of the bulk solution to the total channel resistance can be determined from the conductance in the limit of zero concentration. In this limit, the channel is nearly always empty and the solution reduces to that of the classical Nernst–Planck equation. Table I shows the ratio of the conductance for three different channel lengths relative to the conductance when the total channel length (L) is equal to the physical channel length (M), i.e., no bulk solution. It can be seen that the bulk solution represents a major component of the total resistance (determined when there is 16 Å of bulk solution), ranging from 58 to 90% of the total resistance for the different channels. Most of the resistance lies within the first 8 Å of the bulk solution since increasing the bulk solution from 8 to 16 Å only decreased the resistance by ~10%. For this reason, it is assumed in the following calculations that the total "channel" consists of the physical channel plus 8 Å of bulk solution at each end.

Fig. 3 shows the potential energy profiles for the three channels. Shown are the Born image potential (U_B) and the potential from the fixed charge in the center of the channel (U_F); and the energy of interaction (U_I) and the total energy (U_T) when a second ion is in the center of the channel. For the case where $z_f = -1$, U_I and U_F are just equal and opposite to each other. For these channels, the Born image potential is small compared with the other forces. Shown in the figures are the potential at low

TABLE I
DEPENDENCE OF CONDUCTANCE (G) ON LENGTH OF INCLUDED BULK SOLUTION ($L - M$)

Channel	$G(L)/G(L = M)$		
	$L = M$	$L = M + 8$ Å	$L = M + 16$ Å
$M = 8$ Å, $z_f = -1$	1.0	0.33	0.30
$M = 8$ Å, $z_f = -1.5$	1.0	0.12	0.10
$M = 16$ Å, $z_f = -1$	1.0	0.45	0.42

L, total channel half length; M, physical channel half length; $C \to 0$.

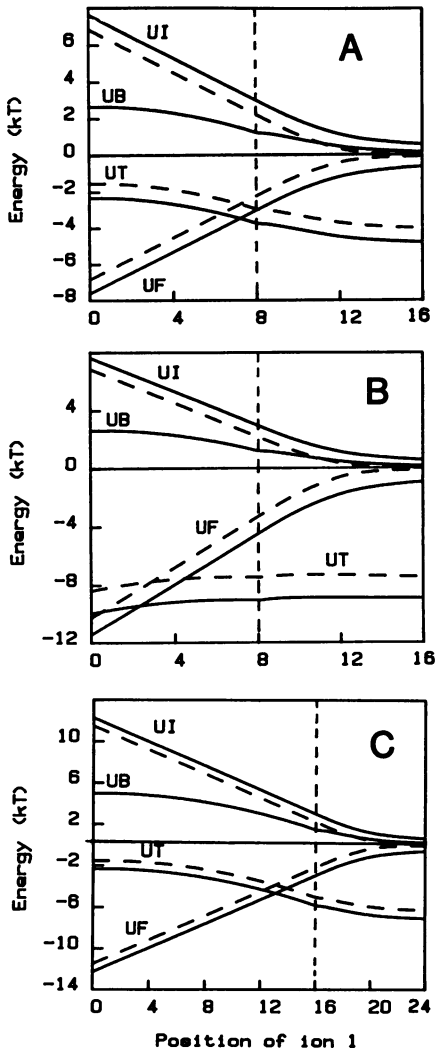

FIGURE 3 Profile for zero concentration (——) and for $C = 2.6\ M/L$ (---) of the Born image potential (UB) and fixed charge potential (UF) when there is one ion in the channel; and of the interaction potential (UI) and total potential (UT) when there are two ions in the channel (ion two located at $X = 0$), shown for three different channels (radius, 4 Å): (*A*) physical length ($2M$) = 16 Å, total length ($2L$) = 32 Å, fixed charge (z_f) = −1; (*B*) $2M = 16, 2L = 32, z_f = -1.5$; (*C*) $2M = 32, 2L = 48, z_f = -1$. The dotted line at 8 or 16 Å indicates the end of the physical channel.

($C = 0$) and high ($C = 2.6\ M/L$) concentrations. There is a small but significant reduction of the potentials at high concentration due to the Debye–Huckel screening. (By assumption, U_B is concentration independent.)

As can be seen in Fig. 3, there is a kink in the Born potential energy (U_B) curve at $X = M$, corresponding to a discontinuity in the Born force. This arises from the discontinuity in the derivative of $K(x)$ (Eq. 27). In addition, there is a discontinuity in the fixed charge force at $X = 0$ and in the interaction force at $X_1 = X_2$. Also, the derivatives of S and S_e are discontinuous at $X = M + a$. These discontinuities require some special care in the numerical solution (see Appendix).

The flux for the general case (referred to as the "two-ion" model) will be compared with the results for the case where the channel can be occupied by at most one ion ("one-ion" model). The one-ion case, which has a simple analytical solution (see Appendix), was recently introduced by Levitt (1986) as a useful approximation for modeling biological channels. Fig. 4 shows the one-ion and two-ion conductance for an applied voltage of 25 mV as a function of the concentration along with the probability that there are zero, one, or two ions in the two-ion channel. The one-ion model provides a fair approximation (underestimating the flux at high concentrations by ~30%) for a fixed charge (z_f) of −1, but a poor approximation (only 14% of the two-ion flux) for a fixed charge of −1.5.

The failure of the one-ion model for a fixed charge of −1.5 provides qualitative insight into important features of the two-ion model. At high concentrations, there is a high probability that one ion is near the fixed charge in the center of the channel while the position of the second ion is determined by the balance between the attractive fixed charge force and the repulsive interaction and image forces. For $z_f = -1$, the fixed charge and interaction forces cancel each other out and the minimum in the total potential (U_T, Fig. 3 *A*) and, therefore, the likely position of the second ion is at the channel ends where it will have only a small influence on the ion in the channel center. Since the channel conductance is determined primarily by the rate the ion in the channel center can climb out of the potential well, the second ion will have little effect on the conductance for $z_f = -1$, even at high concentrations. However, for the case where $z_f = -1.5$, the attractive force from the fixed charge is greater than the repulsive interaction potential, and the minimum in the total energy (Fig. 3 *B*) occurs when both ions are near the channel center. In this case there will be a strong interaction between the two ions, greatly increasing the flux at high concentrations. This effect is shown more quantitatively in Fig. 5. Here, the total energy as a function of the position of the ion is shown for two cases: (*a*) when there is only one ion in the channel and (*b*) when there is a second ion located 2 Å to the left of the center of the channel. This second case corresponds to what might be expected at high concentrations for $z_f = -1.5$. The energy profiles in Fig. 5 correspond to the potential barrier that the ion must pass to leave the channel. It can be seen that the presence of the second ion greatly lowers the height of this barrier (from $8kT$ down to $3kT$). This reduction in barrier height explains why the flux for the two-ion model is about seven times that for the one-ion model at high concentrations for $z_f = -1.5$.

Qualitatively, this difference between a fixed charge of −1 and −1.5 is expected because a channel with a fixed charge of −1 should have a low probability of having more than one ion in the channel (not including the bulk solution region) and therefore can be approximated by the one-ion model. One can extrapolate from these results to the question of the range of validity of the two-ion model

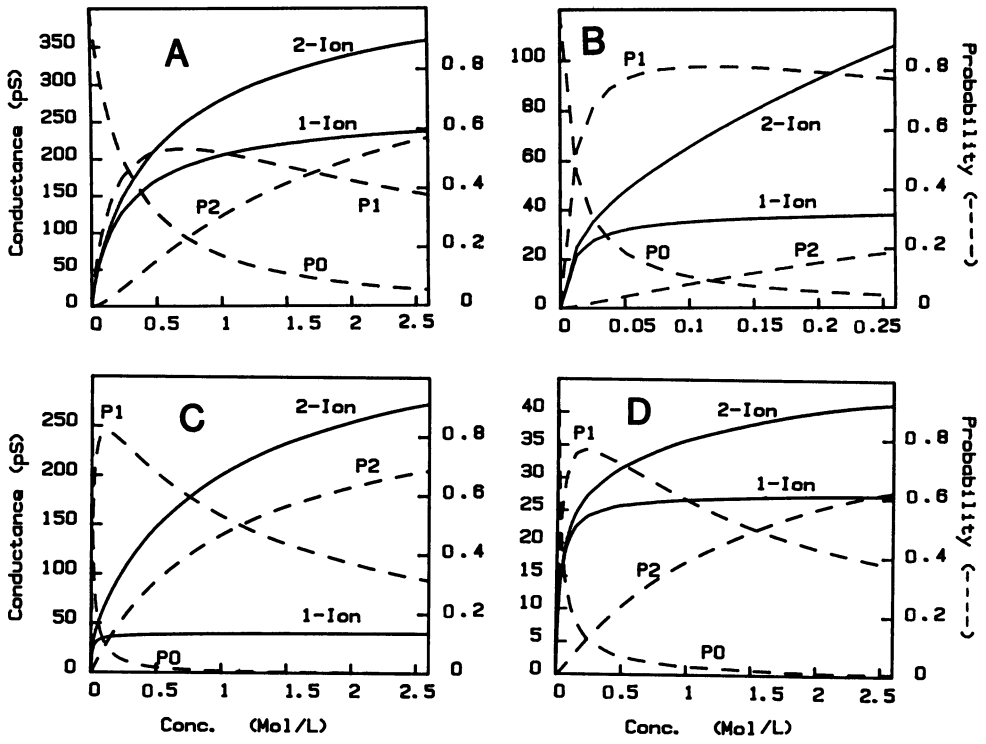

FIGURE 4 Conductance (picoSiemons) and probability that there is zero (P0), one (P1), or two (P2) ions in the two ion channel as a function of concentration. The solution for the two-ion channel is compared with the analytical solution for the one-ion channel (Eq. 19A). The results are shown for the three channels: (*A*) $2M = 16$ Å, $z_f = -1$; (*B* and *C*) $2M = 16$, $z_f = -1.5$; (*D*) $2M = 32$, $z_f = -1$.

developed here. One would expect that the two-ion model should be valid if the channel region has a low probability of being occupied by more than two ions. This suggests that the two-ion model should be valid for a fixed charge of two or less for the channel model used here.

The voltage dependence of the flux for the $M = 16$ Å channel is shown in Fig. 6. In the limit of low concentration, the current–voltage relation is sub-ohmic, whereas at high concentrations ($C = 2.6\ M/L$) it becomes supra-ohmic. The voltage dependence of the one-ion model is nearly identical to that of the two-ion model.

DISCUSSION

This two-ion continuum solution is completely general and, in theory, can be applied to any channel, given the energy profile (including the interaction between ions), cross-sectional area, and diffusion coefficient. For example, it could be used to model the no pass or single file conditions that occur in narrow channels by introducing a strong interaction potential that kept the ions at a fixed distance. However, for both theoretical and practical reasons, it is best suited for situations where the forces are relatively long range and slowly varying, such as the electrostatic forces in this paper. Theoretically, the continuum approach requires a clear separation between the long range forces that enter through the potential energy term (w) and the short range collisional forces that enter through the diffusion coefficient (D) (Levitt, 1986). Practically, an accurate numerical solution requires that the differential equation be solved on a mesh that is fine compared with the distance

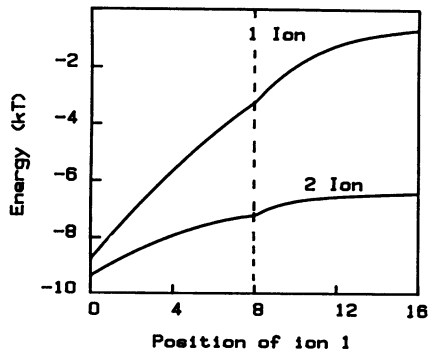

FIGURE 5 Energy of ion one as its position varies from $X = 0$ (center) to $X = 16$ Å (end). The energy when there is just one ion in the channel is compared with the case when there are two ions, with ion two located at $X = -2$ Å. ($2M = 16$, $z_f = -1.5$).

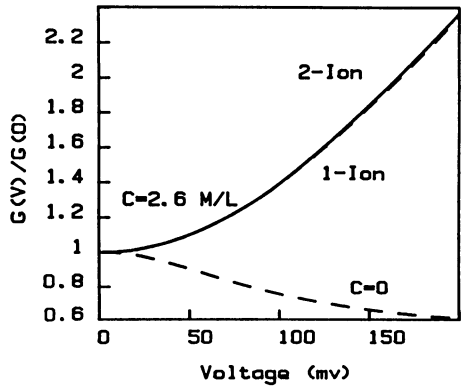

FIGURE 6 Conductance at voltage $V[G(V)]$ relative to zero voltage conductance $[G(0)]$ as a function of applied voltage (millivolt) at low ($C = 0$) and high ($C = 2.6\ M/L$) concentrations. ($2M = 32$, $z_f = 1$).

over which there are significant changes in the energy. Steep energy barriers require a much greater number (N) of grid points, leading to increased computer time and storage (both of which increase as N^2). For example, the gramicidin channel is thought to have relatively large, short range barriers (of unknown origin) at the channel mouth. For such a barrier, the continuum approach has no theoretical advantage over the much simpler reaction rate approach. Gramicidin is probably better described by a hybrid approach in which the reaction-rate theory is used to model the channel ends and the continuum approach is used to model the movement of the ion in the slowly varying (and better characterized) energy barrier in the center of the channel (Levitt, 1982).

The general continuum approach is ideally suited for situations where a significant fraction of the total resistance of the channel is contributed by diffusion in the bulk solution at the channel mouth. For example, in the channels considered here, up to 90% (see Table I) of the resistance (at low concentrations) is in the bulk solution. In addition the forces in the bulk solution result primarily from long range, well understood, electrostatic forces, and the diffusion coefficient should be close to that for bulk water. For these reasons the continuum solution obviously represents the best approach to modeling this region.

There is a class of K^+-selective channels (Maxi-k^+) that have very high maximum conductances (200–400 pS) (Latorre and Miller, 1983). These conductances are so large that the bulk solution must contribute to the total resistance. Thus, an accurate model of these channels requires some type of continuum approach. The short channel ($2M$ = 16 Å, $z_f = -1$, Fig. 4 *A*) discussed above has an absolute conductance and concentration dependence that is similar to that seen for the Maxi-K^+ channels, indicating, at least, that a continuum channel with these dimensions could be a model for these channels. The long channel (Fig. 4 *D*, $2M$ = 32 Å, $z_f = -1$) has dimensions similar to those of the narrow region of the acetylcholine receptor channel (Brisson and Unwin, 1985), and the absolute value and concentration dependence of the conductance (Fig. 4 *D*) are similar to the experimental values (Dani and Eisenman, 1987), indicating that this might also be a useful model for the acetylcholine channel.

Although the mathematical derivation is quite involved, the solution is basically simple, requiring <10 s on a large computer (for $N = 48$). Once the solution has been obtained for one case, it can be applied to any other case simply by modifying the energy functions. The major limitation of this solution is the requirement that the channel can be occupied by at most two ions. This requirement is relaxed somewhat by including the influence of the Debye–Huckel reaction field in the bulk solution, which, in effect allows for the presence of an (unlimited) number of additional ions that, however, must be at equilibrium. As discussed above, extrapolation from the results of comparing the one-ion and two-ion models suggests that the two-ion model should be satisfactory if the fixed charge valence is not greater than two. The theoretical approach developed here for the two-ion model can be extended in an analogous way to allow for three or more ions.

APPENDIX

Derivation of the Electrostatic Energy and Restricted Area Functions for a Cylindrical Channel

Potential Energy of Ion–Ion Interaction. If one knows the electrical potential $\phi(x_1, x)$ at x when another ion is at x_1 (valance z), then the interaction potential $u_1(x_1, x)$ is simply $z\phi(x_1, x)$. The field lines are assumed to have the form shown in Fig. 1 with the cross-sectional area described by Eq. 26. The field at the position of the ion (x_1, assumed to ≥ 0) is defined to be E_0. In region II, no other ions are present, so that, from Gauss's law, the E field (in dimensionless terms) at any position x is described by

$$\xi_{\pm}(x) = (x) = 2\pi z_1[\alpha(x_1) \pm 1]/s(x)$$

$$\alpha(x_1) = \xi_0 s_0/(2\pi z_1), \quad (1A)$$

where the + and − refer to the right and left side of x_1, respectively.

In regions I and III, the potential is described by the Debye–Huckel equation:

$$(S\Phi')' = -(4\pi e/\epsilon_w) \sum_i z_i C_i S_e^i, \quad (2A)$$

where the summation is over all the ions present and S_e^i is the restricted area available to the ion and is assumed to be equal to S in these regions, which are removed from the pore mouth by a distance of at least a. It is also assumed that only monovalent ions are present ($z_i = \pm 1$). The concentration of the background ions are assumed to be in equilibrium:

$$C_{\pm}/C_0 = e^{\mp e\Phi/kT} \simeq 1 \mp e\Phi/kT. \quad (3A)$$

The expansion in the second equality of Eq. 3A should be valid because variations in potential in these regions should be small. Since the surface area is spherical, these equations are exactly analogous to those used in the Debye–Huckel treatment (McQuarrie, 1976) and has the solution (expressed in dimensionless variable):

$$\phi_I = B_I e^{\lambda(x+m)}/(x+m); \Phi_{III} = B_{III} e^{-\lambda(x-m)}/(x-m), \quad (4A)$$

$$\lambda^2 = 8\pi\gamma c_0$$

where λ is the Debye constant. The constants B_I and B_{III} are determined from the condition that E must be continuous at the boundary between regions I and III (obtained from the derivative of Eq. 4A) and region II (Eq. 1A):

$$\phi_I = \frac{z_1(\alpha - 1)e^{\lambda(x+1+m)}}{(1+\lambda)(x+m)}; \phi_{III} = \frac{z_1(1+\alpha)e^{-\lambda(x-1-m)}}{(1+\lambda)(x-m)}. \quad (5A)$$

Eq. 5A gives the potential in regions I and III. The potential in region II is obtained by integrating over the E field (Eq. 1A). Also, the value of α is obtained from the condition that the potential at x_1 must be the same whether approached from the left or right. Carrying out these manipulations, the final expression for $u_1(x,y)$ is obtained. It is described by Eq. 27C in the text.

Fixed Charge Potential Energy (U_F). For the calculations in this paper it is assumed that the fixed charge (valence z_f) is in the center of the channel ($x = 0$) so that the potential energy of an ion at x can be obtained immediately from u_I (see Eq. 27):

$$u_F(x) = u_I(0, x) = 2z_f z I(|x|). \tag{6A}$$

This calculation assumes that the field lines from the fixed charge have the form shown in Fig. 1, even in the center of the channel where the fixed charge is located. This is obviously incorrect for a fixed point charge. However, if the fixed charge resembles a ring of partial charges then this approximation should be satisfactory.

Born Image Potential Energy (U_B). As is customary in this calculation the diffuse charge component will be neglected ($\lambda = 0$). The image potential is defined as the extra energy required to charge up the ion when it is in the channel compared with when it is in the bulk solution. In the homogeneous bulk aqueous solution, the field (ξ_H) is described by

$$E_H = q/(\epsilon_\omega X^2) \quad \xi_h = n/x^2 \quad n = q/e. \tag{7A}$$

For the ion in the channel, the field far from the ion is described by the equations derived above (Eq. 1A and the derivative of Eq. 5A) for the ion interaction energy. This field must be modified as one approaches the ion and this is approximated by adding to the far field expression a short-range term defined by

$$\xi_s(x) = \begin{cases} 0 & |x - x_0| \geq c \\ \xi_h(x) - \xi_h(c) & c \leq |x - x_0| \end{cases}$$

$$c = \begin{cases} 1 & |x_0| \leq m \\ 1 + x_1 - m & |x_0| \geq m, \end{cases} \tag{8A}$$

where ξ_h is given by Eq. 7A and x_0 is the position of the ion. This form was chosen primarily for its simplicity. It has the expected property that as one approaches close to the ion the field becomes equal to the homogeneous field, while at a long distance (one pore radius in the channel and a larger radius outside the channel) it becomes zero. The image potential is defined as the extra potential at the ion center due to the presence of the ion channel:

$$\phi_B = 2n[\alpha(x_0) + 1]I(x) + \int_0^c [\xi_h(x) - \xi_h(c)]dx - \int_0^\infty \xi_h(x)dx$$
$$= 2n[\alpha(x_0) + 1]\, I(x) - 2n/c. \tag{9A}$$

The first term in Eq. 9A is the long-range contribution (see Eq. 27c), the second is the integral of the short-range field and the third is the potential in the homogeneous bulk solution. The Born image potential energy is then the energy required to charge up the ion against this potential:

$$u_B = \int_0^z \phi_B(n)dn = z^2\{[1 + \alpha(|x|)]I(|x|) - K(|x|)\}$$

$$K(x) = \begin{cases} 1 & |x| \leq m \\ (1 + x - m)^{-1} & m \leq |x|. \end{cases} \tag{10A}$$

Applied Potential (ψ). This refers to the spatial dependence of the applied potential. From Gauss's law, the potential is described by the differential equation (see Eqs. 2A–4A):

$$(s\psi')' = \begin{cases} 0 & |x| \leq m + 1 \\ \lambda^2 s\psi & m + 1 \leq |x|. \end{cases} \tag{11A}$$

The potential profile is then obtained by solving Eq. 11A subject to the boundary condition that $\psi_1 = \psi 1$ at $x = -\infty$ and $\psi = 0$ at $x = \infty$:

$$\psi(x)/\psi_1 = \begin{cases} I(x)/2I(0) & x \geq 0 \\ 1 - I(-x)/2I(0) & x \leq 0. \end{cases} \tag{12A}$$

Restricted Area Available to Ion (s_e). This is the correction for the finite size of the ion (radius B) and corresponds to the area available to the center of the ion. Fig. 7 shows how this area is defined for the different regions of the cylindrical channel. For $-m \leq x \leq m$, s_e is obtained immediately from the cross-sectional area available to the ion ($s_e = S_e/a^2$, $b = B/a$):

$$S_e = \pi(a - B)^2; \; s_e = \pi(1 - b)^2. \tag{13A}$$

In the region $m \leq |x| \leq m + 1$, the total surface area (s) is equal to (see Fig. 7):

$$s = 2\pi r^2[1 - \cos(\theta)] = 2\pi rh$$
$$h = x - m; \quad r = (1 + h^2)/2h; \quad \cos(\theta) = 1 - h/r. \tag{14A}$$

The restricted area is the region of spherical surface subtended by the reduced angle θ':

$$s_e = 2\pi r^2\,[1 - \cos(\theta')]$$
$$\theta' = \theta - \phi; \quad \sin(\phi/2) = b/2r. \tag{15A}$$

Eqs. 14A and 15A can be solved for r, θ, and ϕ, providing an exact solution for the restricted area (S_e). This exact expression can be approximated by the following (simpler) expression:

$$s_e = \pi[(1 - b)^2 + h^2(1 - b^2)], \; h = x - m. \tag{16A}$$

This approximation is quite good, deviating from the exact result by <5% for $b = 0.5$. In the region $m + 1 \leq |x|$, s_e will be approximated by

$$s_e = 2\pi h^2 - 2\pi hb = 2\pi h(h - b). \tag{17A}$$

These expressions for s_e (Eqs. 13A, 16A, and 17A) are continuous across the three regions. It has been assumed in this derivation that the physical radius (a_p), which should be used in Eq. 13A, is equal to the electrostatic pore radius (a). If, as seems likely, a_p is less than a, then the expression for b can be modified as follows:

$$S_e = \pi(a_p - B)^2 = \pi(a - B')^2; \quad B' = B + a - a_p$$
$$s_e = S_e/a^2 = \pi(1 - b)^2; \quad b = (B + a - a_p)/a. \tag{18A}$$

Using Eq. 18A for b should provide an approximate correction for the inequality of a and a_p.

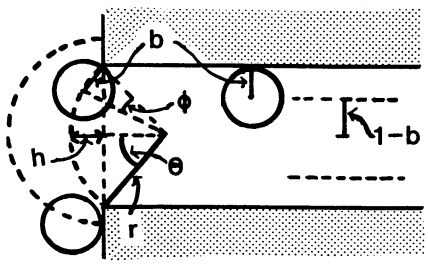

FIGURE 7 Diagram illustrating relations used in calculation of restricted area (S_e). The dimensionless pore radius is 1 (normalized by a) and the dimensionless ion radius is b ($=B/a$).

Classical Nernst–Planck, One-Ion and No Interaction Two-Ion Solution

Simple analytical expressions can be obtained for these three cases which are given here for reference. The solution to the classical Nernst–Planck equation is described by (Levitt, 1986):

$$J^N = (C_1 e^{\psi_1} - C_2)/I(L); \quad I(X) = \int_{-L}^{X} D^{-1} H_1^{-1} dX, \quad (18A)$$

where (see Eq. 5)

$$H_1 = S_e(X) e^{-w}.$$

Also, the concentration at X, $C^N(X)[=p_1(X)]$ can be written as

$$C^N(X)/C_1 = e^{-w(x)}[e^{\psi_1} + (C_2/C_1 - e^{\psi_1})\, I(X)/I(L)]. \quad (19A)$$

This assumes that the concentration at the channel ends ($-L$ and L) is in equilibrium with the bulk solution.

For the case where the channel can be occupied by at most one ion, the flux is described by (Levitt, 1986):

$$J^1 = P_0 J^N; \qquad P_0 = [1 + C_1 Q]^{-1},$$

$$Q = \int_{-L}^{L} S_e(C^N/C_1) dX, \quad (19A)$$

where C_1 is in units of No./cm^3. This is the "one-ion" solution for the flux that is compared with the general "two-ion" flux in the figures.

The differential equation for the two-ion case can be solved analytically for the case where there is no interaction between ions ($U_1 = 0$; $h(x, y) = h_1(x)h_1(y)$). Then, $f(x, y)$ can be written in the form $f_1(x)f_1(y)$ and Eq. 18a reduces to

$$h(x) \frac{df_1}{dx} = \text{constant}. \quad (20A)$$

This relation also satisfies the boundary condition, Eq. 18c. Writing $f(x, y)$ in the form:

$$f(x, y) = Kf(-\ell, x) f(-\ell, y). \quad (21A)$$

The constant K can be determined from the boundary condition Eq. 18b:

$$K = (C_2/C_1)\, e^{-\psi_1} = \beta. \quad (22A)$$

Integrating Eq. 20A from $-\ell$ to x:

$$f(-\ell, x) = (C_1/C_2)e^{\psi_1} + [1 - (C_1/C_2)e^{\psi_1}] I(x)/I(\ell)$$
$$= e^{w}\, C^N(x)/C_2. \quad (23A)$$

From this solution for f, the final expression for the no interaction (NI) flux can be obtained, written in terms of the classical Nernst flux (Eq. 18A) and concentrations (Eq. 23A):

$$J^{NI} = J_1^{NI} + J_2^{NI}$$

$$J_1^{NI} = P_0 J^N; \qquad J_2^{NI} = P_0 J^N \int_{-L}^{L} S_e(x) C^N(X) dX,$$

where P_0 is the probability the channel is empty and is obtained from the integral over f (see Eqs. 19 and 20).

Details of Numerical Solution

The equations are solved by the conventional finite difference method. The function $f(x, y)$ is represented by the discrete values of f_{ij} where i goes from 0 to $n - 1$ and j goes from $i + 1$ to n (the term f_{jj} is eliminated by the boundary condition, Eq. 18d, $f_{j-1,j} = f_{jj}$). The differential Eq. 18a then becomes a difference equation which can be written in the form

$$A^1_{i-1,j} f_{i-1,j} + A^2_{i,j-1} f_{i,j-1} + A^3_{i,j} f_{i,j}$$
$$+ A^4_{i,j+1} f_{i,j+1} + A^5_{i+1,j} f_{i+1,j} = 0 \quad (25A)$$

for $i = 0$ to $n - 1$, $j = i + 1$ to n. The terms $f_{-1,j}$ and $f_{i,n+1}$ (that appear in the $(0, j)$ and (i, n) equation, respectively) must be eliminated to get a closed solution. Eq. 18b is used to eliminate $f_{i,n+1} = \beta f_{-1,i}$. These relations are then substituted in the second boundary condition (Eq. 18c) to eliminate $f_{-1,j}$. This leads to a set of equations for $i = 0$ and $j = i+1$ to $n-1$:

$$B^1_{i-1} f_{0,i-1} + B^2_i f_{0,i} + B^3_{i+1} f_{0,i+1} + B^4_i f_{1,i} + B^5_i f_{i,n-1} = 0, \quad (26A)$$

along with Eqs. 25A for $i=1$ to $n-2$, $j=i+1$ to $n-1$. In addition, Eqs. 18e provide the only points where definite value of f_{ij} are prescribed:

$$f_{0,n} = 1; \qquad f_{0,0} = 1/\beta; \qquad f_{n,n} = \beta. \quad (27A)$$

This then yields a set of $N = (n-2)(n+1)/2+1$ equations in N unknowns that is solved by use of the Yale Sparse Matrix Program.

Some of the potential (Eq. 27) and area (Eq. 29) functions have discontinuities in their first derivative (which enter the coefficients of the sparse matrix and the expression used to determine the flux [Eq. 25]). To minimize the influence of these discontinuities the grid points were chosen so that they fell on the points of discontinuity and the derivative was assigned the average of the values on each side of the point.

Received for publication 6 November 1986 and in final form 10 April 1987.

REFERENCES

Brisson, A., and P. N. T. Unwin. 1985. Quaternary structure of the acetylcholine receptor. *Nature (Lond.).* 315:474–477.

Dani, J. A., and G. Eisenman. 1987. Monovalent and divalent ration permeation in acetylcholine receptor channels. *J. Gen. Physiol.* 89:959–983.

Hageman, L. A., and D. M. Young. 1981. Applied Iterative Methods. Academic Press, Inc., New York.

Jordan, P. C. 1982. Electrostatic modeling of ion pores: energy barriers and electric field profiles. *Biophys. J.* 39:157–164.

Jordan, P. C. 1984. The total electrostatic potential in a gramicidin channel. *J. Membr. Biol.* 78:91–102.

Latorre, R., and C. Miller. 1983. Conduction and selectivity in potassium channels. *J. Membr. Biol.* 71:11–30.

Levitt, D. G. 1978. Electrostatic calculations for an ion channel. I. Energy and potential profiles and interactions between ions. *Biophys. J.* 22:209–219.

Levitt, D. G. 1982. Comparison of Nernst-Planck and reaction-rate models for multiply occupied channels. *Biophys. J.* 37:575–587.

Levitt, D. G. 1985. Strong electrolyte continuum theory solution for equilibrium profiles, diffusion limitation, and conductance in charged ion channels. *Biophys. J.* 48:19–31.

Levitt, D. G. 1986. Interpretation of biological flux data: reaction-rate versus continuum theory. *Annu. Rev. Biophys. Chem.* 15:29–57.

McQuarrie, D. A. 1976. Statistical Mechanics. Harper and Row, New York.

Saad, Y. 1982. Practical use of some Krylov subspace methods for solving indefinite and unsymmetric linear systems. Technical report No. 214. Yale University, Department of Computer Science.

Young, D. M., and K. C. Jea. 1980. Generalized conjugate-gradient acceleration of nonsymmetrizable iterative methods. *Lin. Alg. App.* 34:159–194.